Electron cyclotron resonance etching of semiconductor structures studied by *in-situ* spectroscopic ellipsometry

Suraiya Nafis[a], Natale J. Ianno[a], Paul G. Snyder[a], William A. McGahan[a,b], Blaine Johs[b] and John A. Woollam[a,b]

[a]*Center for Microelectronic and Optical Materials Research, and Department of Electrical Engineering, University of Nebraska, Lincoln, NE (USA)*

[b]*J.A. Woollam Co., 650 J Street, Lincoln, NE (USA)*

Abstract

The motivation for this work was to develop *in-situ* monitoring and control of electron cyclotron resonance (ECR) as an anisotropic etch doing minimal surface damage to electronic materials. We have used a modular rotating-analyzer spectroscopic ellipsometer in both the *in-situ* and *ex-situ* modes to investigate etching of Si, SiO_2, GaAs and InP, as well as GaAs/$Al_{1-x}Ga_xAs$/GaAs and InP/$In_{1-x}Ga_xAs$ heterostructures. Etching was done using a 175 W ECR source with mixtures of CCl_2F_2 and either oxygen or inert gases in various flow ratios in order to prevent polymerization. The experimental variables in these experiments were the gas ratios, gas species, r.f. substrate bias voltage (power) and substrate temperature. Etching was found to create a thin damage region near the surface modeled ellipsometrically as crystalline-plus-amorphous semiconductor in a Bruggeman effective-medium mixture.

1. Introduction

There is considerable interest in electron cyclotron resonance (ECR) as a high density source for anisotropic dry etching, and minimal surface damage for production of submicron-sized features [1]. In order to understand and control this process a non-destructive *in-situ* method is highly desirable, and spectroscopic ellipsometry (SE) is ideal for this application [2].

In this paper we describe SE experiments in which frequent complete spectral scans from 300 to 800 nm were taken. Also data were taken in real time *in situ* at a few optimally selected wavelengths as etching proceeded [2].

2. Experimental details

The following materials and structures were used: Si, GaAs, and InP bulk grown and polished crystals; thermally grown SiO_2 on Si, GaAs/(30 wt.% Al–Ga–As)/GaAs and (53 wt.% In–Ga–As)/InP epitaxially grown structures all with (100) orientation. Optical constants were obtained from the literature for Si [3], GaAs [4], InP [3], amorphous SiO_2 [3], amorphous silicon (a-Si) [3], amorphous GaAs (a-GaAs) [5], GaAs oxide and InP oxide [6]. Amorphous InP optical constants were not available; so those of a-GaAs were substituted.

The ECR source was operated in a cryopumped chamber with a base pressure of 5×10^{-7} Torr. The end of the 175 W ECR source was 15 cm from the substrate surface and at an angle of 45° to the normal.

The rotating-analyzer ellipsometer was mounted on stress and birefringent-free Studna windows at an angle of incidence of 70°. (This angle was chosen to accommodate optimal *in-situ* monitoring of dielectric depositions. The optimal angle for semiconductors is near 75°.) The substrate was water cooled, and an r.f. bias was applied to the metallic back plate isolated by ceramic from the sample.

The etching gas selected was CCl_2F_2 since it etches a wide range of materials. Oxygen or hydrogen is mixed with CCl_2F_2 to prevent polymerization on the substrate [7]. Thus the flow rates of 2 standard $cm^3\,min^{-1}$ for CCl_2F_2 and 6 standard $cm^3\,min^{-1}$ for O_2 (or H_2) were held constant, and the main parameter of the etch was the r.f. bias.

A commercial atomic force microscope was used, capable of "remote" operation and with unusually shaped samples. This yielded top views (two-dimensional plots), as well as three-dimensional views and statistical analysis of peak height variation and r.m.s. roughness.

3. Results

3.1. SiO_2/Si

The starting oxide thickness was 410.5 nm, and etching in CCl_2F_2 with oxygen etched SiO_2 at a rate of up

0040-6090/93/$6.00

to 17 nm min^{-1}, depending on the r.f. bias power (30 or 40 W), gas pressure (6 mTorr) and species (O_2 or H_2). SiO_2 etched up to three or four times more rapidly in H_2 mixtures than in O_2 mixtures.

3.2. Bulk crystalline Si, GaAs and InP

Etching was done only with CCl_2F_2 and O_2 with 20 W r.f. bias at a pressure of 1 mTorr and 175 W, and etch rates were in the range from 2.0 to 3.5 nm min^{-1} as determined by masking and profilometry after completion of experiments. *In-situ* ellipsometry on thick bulk materials does not determine thicknesses; however, surface effects are seen which could be generally due to roughening, oxide thickness or damage layer formation. Figure 1 shows models used for fitting of full SE data on Si, GaAs and InP before etching, and Fig. 2 shows models which fit the data after etching.

Note in Fig. 1 that the natural oxide thicknesses are on the order of 1.8–3.2 nm. Etchants include oxygen, and Fig. 2 shows that the oxides thicken to 2.5–4.3 nm during etching and mix with amorphous semiconductor. In addition a damage layer is created which is modeled ellipsometrically by adding 50% (fixed) amorphous material to crystalline material [8]. The final best-fit models for the ellipsometric data are given in Fig. 2 together with the biased estimator errors [9]. These errors are low, and the fits are excellent, except for InP, indicating an imperfect model for this case.

1 EMA SiO_2 / 20% a-Si	1.76 nm	
0 Si		$\chi^2 = 0.79$
(a)		
1 EMA GaAs Ox / 13% a-GaAs	2.81 nm	
0 GaAs		$\chi^2 = 0.60$
(b)		
1 EMA InP Ox / 6% a-GaAs	3.16 nm	
0 InP		$\chi^2 = 0.94$
(c)		

Fig. 1. Models used for the ellipsometric analysis of bulk substrates before etching together with biased estimator errors. Typical oxide layer thickness uncertainties are ± 0.1 nm.

2 EMA SiO_2 / 33% a-Si	2.47 nm	
1 EMA Si / 50% a-Si	0.97 nm	
0 Si		$\chi^2 = 0.97$
(a)		
2 EMA GaAs Ox / 19% a-GaAs	3.59 nm	
1 EMA GaAs / 50% a-GaAs	0.71 nm	
0 GaAs		$\chi^2 = 0.96$
(b)		
2 EMA InP Ox / 9% a-GaAs	4.32 nm	
1 EMA InP / 50% a-GaAs	0.65 nm	
0 InP		$\chi^2 = 1.71$
(c)		

Fig. 2. Models used for the ellipsometric analysis of bulk materials after etching, together with biased estimator errors. Typical damage layer thickness uncertainties are ± 0.1 nm.

3.3. Multilayer structures

Variable-angle spectroscopic ellipsometry has been enormously effective in determining layer thicknesses and alloy fractions in multilayer heterostructures [10]. Typically these thicknesses are accurate to better than 0.5 nm and confirmed by cross-sectional transmission electron microscopy [11]. Optical constants are now known for $Al_xGa_{1-x}As$ [12, 13] alloys, and $In_{0.53}Ga_{0.47}As$ [14] and strained layers at other compositions [15]. Thus considerable microstructural analysis can be done by SE, including in an *in-situ* environment. With multilayer structures, thicknesses and compositions can be simultaneously monitored in real time. Considerable data were taken during etching in the experiments at present reported, with intermittent stops to make full spectral scans. Typical *in-situ* data were taken during etching at 350, 450, 550 and 650 nm wavelengths every few seconds. Owing to space limits in this paper, these results will be discussed elsewhere.

Figure 3 shows spectral data after etching on an $In_xGa_{1-x}As$ layer in CCl_2F_2/O_2 from an initial 77–45.4 nm thickness for the $In_xGa_{1-x}As$/InP sample. An interesting trend is found; the composition increased from its initial $In_{0.5}Ga_{0.5}As$ to $In_xGa_{1-x}As$ with x in the range between 0.55 and 0.60 soon after etching started. Presumably this increase in x is due to preferential etching of Ga by the etchants used for these experiments.

As for the bulk material case, etching GaAs/$Al_xGa_{1-x}As$/GaAs resulted in a rapid increase in oxide thickness to approximately 4–5 nm from an initial value near 2 nm.

4. Discussion

We have shown that *in-situ* SE is sensitive to surface chemistry and surface damage during etching of semiconductors. The ECR and particular etchants used in these experiments are shown to do little surface roughening (as confirmed by atomic force microscopy (AFM)). However, etching creates a damage layer which extends downwards several nanometers from the top surface. One final note is that the SE and AFM data reveal complementary information. There are irregular surface features seen by AFM when the lateral roughness has a bandwidth between 10 nm and 5 μm, and a vertical

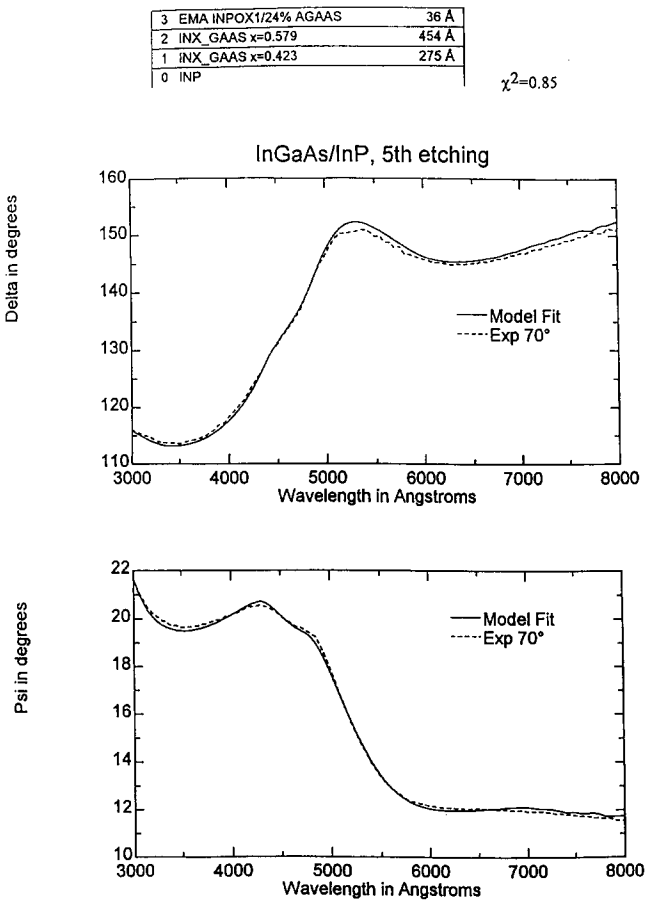

Fig. 3. Spectral Ψ and Δ data for $In_xGa_{1-x}As/InP$ after etching in $CCl_2F_2-O_2$.

roughness down to fractions of a nanometer. Using the effective-medium approximation, SE senses microstructure both at and below the surface to a depth dependent on the optical absorption coefficient when these features have dimensions less than about 100 nm.

Acknowledgments

Research was supported by the US Army Strategic Defense Command Contract DASG60-92-C0028 and Defense Advanced Research Projects Agency Contract DAAH01-92-C-R191.

References

1 J. Asmusson, in S. M. Rossngel, J. J. Cuomo and W. D. Westwood (eds.), *Handbook of Plasma Processing*, Noyes, Park Ridge, NJ, 1990, pp. 285–230.
2 B. Johs, D. Meyer, G. Cooney, H. Yao, P. G. Snyder, J. A. Woollam, J. Edwards and G. Maracas, *Materials Research Society Symp. Proc., Long Wavelength Semiconductor Devices, Materials and Procedures*, Vol. 216, Materials Research Society, Pittsburgh, PA, 1991, p. 459.
3 E. S. Palik (ed.), *Handbook of Optical Constants of Solids*, Academic Press, New York, 1985.
4 G. E. Jellison, Jr., *Opt. Mater., 1* (1992) 151.
5 M. Erman, J. B. Theeten, P. Chambon, S. M. Kelso and D. E. Aspnes, *J. Appl. Phys., 56* (1984) 2664.
6 D. E. Aspnes, G. P. Schwartz, O. T. Gualtiari, A. A. Studna and B. Schwartz, *J. Electrochem. Soc., 128* (1981) 590.
7 S. J. Pearton, F. Ren, J. R. Lothian, T. R. Fullowan, R. F. Kopf, U. K. Chakrabarti, S. P. Hull, A. B. Anderson, R. L. Kostelak and S. S. Pei, *J. Vac. Sci. Technol. B, 9* (1991) 2487.
8 D. E. Aspnes, J. B. Theeten and F. Hottier, *Phys. Rev. B, 20* (1979) 3292.
9 G. E. Jellison, Jr., *Appl. Opt., 30* (1991) 3354.
10 J. A. Woollam, P. G. Snyder, H. Yao and B. Johs, *Proc. Soc. Photo-Opt. Instrum. Eng., 1678* (1992) 246.
11 J. A. Woollam, P. G. Snyder, A. W. McCormick, A. K. Rai, D. C. Ingram and P. P. Pronko, *J. Appl. Phys., 62* (1987) 4867.
12 D. E. Aspnes, S. M. Kelso, R. A. Logan and R. Bhat, *J. Appl. Phys., 60* (1986) 754.
13 P. G. Snyder, J. A. Woollam, S. A. Alterovitz and B. Johs, *J. Appl. Phys., 68* (1990) 5925.
14 D. E. Aspnes and J. J. Stocker, *J. Vac. Sci. Technol., 21* (1982) 413.
15 C. Pickering, R. T. Carline, M. T. Emery, N. S. Garawol and L. K. Howard, *Appl. Phys. Lett., 60* (1992) 2412.